

# Systematic effects in the low-energy behavior of the current SAID solution for the pion-nucleon system

E. Matsinos<sup>\*a</sup>, G. Rasche<sup>b</sup>,

<sup>a</sup>*Institute of Mechatronic Systems, Zurich University of Applied Sciences,  
Technikumstrasse 5, CH-8401 Winterthur, Switzerland*

<sup>b</sup>*Physik-Institut der Universität Zürich, Winterthurerstrasse 190, CH-8057 Zürich,  
Switzerland*

<sup>\*</sup>Corresponding author. E-mail:  
evangelos[DOT]matsinos[AT]sunrise[DOT]ch

---

## Abstract

We investigate the description of the pion-nucleon experimental data at low energy (i.e., below pion laboratory kinetic energy of 100 MeV) on the basis of the current SAID solution (WI08). We demonstrate that, in a self-consistent analysis scheme, the scale factors of the fits based on the Arndt-Roper formula come out independent of the beam energy and ‘cluster’ around the expectation value of 1. We report systematic effects in the low-energy behavior of the WI08 solution. These effects indicate that at least one of the three following assumptions, underlying the WI08 analysis, does *not* hold, namely that: a) the bulk of the data is reliable, b) the electromagnetic effects are correctly accounted for, and c) the isospin invariance in the strong interactions of the  $\pi N$  system is valid.

*PACS:* 13.75.Gx; 25.80.Dj; 25.80.Gn; 11.30.-j

*Key words:*  $\pi N$  system, elastic scattering, charge exchange, partial-wave analysis, isospin invariance

---

## 1 Introduction

The SAID results for the pion-nucleon ( $\pi N$ ) system [1] are widely used as input in numerous works, not only in those studying aspects of the  $\pi N$  interaction. The results represent an optimization of the description of an extensive database (DB) of measurements, ranging from the  $\pi N$  threshold to (pion laboratory kinetic energy  $T$  of) a few GeV. The experimental data are analyzed

via dispersion relations. The SAID phase-shift solution is regularly updated, conveniently appearing online, which facilitates the fast dissemination of any new results. Furthermore, new measurements are frequently communicated to the developers of this platform prior to their formal publication, ensuring that the site remain at the state-of-the-art level on a number of hadronic processes. Regarding the  $\pi N$  interaction, the current SAID solution is known as WI08. This paper examines one aspect of this solution, namely its low-energy behavior. As such, it is expected to be of interest to those who extract important hadronic quantities from the low-energy SAID phase shifts or compare their experimental results to the predictions obtained on the basis of these phase shifts.

Regarding the SAID phase-shift solutions for  $T \leq 100$  MeV, our concerns have already been expressed on several occasions. To start with, one has the impression that new  $\pi N$  measurements enter the SAID DB with little regard for their self-consistency and/or compatibility with the measurements which are already present in the DB. Had the SAID group implemented robust statistics in their analysis, such a strategy would be less problematic; however, their results are obtained with a ‘standard’  $\chi^2$  function (i.e., with the Arndt-Roper formula [2]), and are thus expected to be sensitive to the presence of outliers in the DB (in particular, of *one-sided* outliers). Secondly, the SAID results for  $T \leq 100$  MeV are literally swamped by the measurements at higher energies. In case that the floating of the data sets is permitted (as the case is when the Arndt-Roper formula is used in the optimization), it is unavoidable that the low-energy behavior of the partial-wave amplitudes will be influenced by the measurements acquired at higher energies. Thirdly, the distribution of the normalized residuals, in a self-consistent analysis using a  $\chi^2$  minimization function, must be the normal distribution  $N(\mu = 0, \sigma^2 = 1)$ , where  $\mu$  denotes the mean of the distribution and  $\sigma^2$  its variance. Any effects observed in this distribution (e.g., significant offsets, asymmetry, dependence of the normalized residuals on the independent variables in the problem, etc.) are indicative of problems in the input or in its modeling. We are not aware of any paper from the SAID group where these issues are addressed. Regarding the use of the SAID solution for  $T \leq 100$  MeV, one final remark is that the measurements from the three  $\pi N$  reactions, i.e., from the two elastic-scattering (ES) reactions ( $\pi^\pm p \rightarrow \pi^\pm p$ ) and from the charge-exchange (CX) reaction ( $\pi^- p \rightarrow \pi^0 n$ ), are forced into an isospin-invariant analysis framework. Evidently, the SAID group choose to disregard the possibility of the violation of the isospin invariance in the hadronic part of the  $\pi N$  interaction<sup>1</sup> at low energy, which has been promulgated by some works during the past two decades [3,4,5].

---

<sup>1</sup> In the following, ‘isospin invariance in the  $\pi N$  interaction’ will be used as the short form of ‘isospin invariance in the hadronic part of the  $\pi N$  interaction’. It is known that the isospin invariance is violated in the electromagnetic (EM) part of the scattering amplitude.

## 2 Method

### 2.1 Low-energy parameterizations of the hadronic $K$ -matrix elements

The presumptions in analyses employing the  $K$ -matrix parameterizations of this section relate to: a) the number of terms which one retains from the original infinite power series (expansion of the hadronic  $K$ -matrix elements in terms of a suitable variable, e.g., of the pion kinetic energy  $\epsilon$  in the center-of-mass (CM) system), and b) the forms used in the modeling of the resonant contributions. In both cases, we are confident that our modeling captures the details of the physical system. Such an approach ensures that the detection of any outliers in the input DBs cannot be attributed to the inability of these parametric forms to account for the energy dependence of the hadronic phase shifts; as a result, the detection of outliers in the fits is indicative of experimental discrepancies.

In the analysis of the low-energy  $\pi N$  measurements using the  $K$ -matrix parameterizations, we retain terms up to (and including)  $\epsilon^2$ . Experience has shown that the coefficients of higher orders in the expansion of the  $K$ -matrix elements cannot be determined from the available measurements at low energy.

#### 2.1.1 Fits to our low-energy $\pi^+p$ database using the $K$ -matrix parameterizations

For  $\pi^+p$  ES, the  $s$ -wave phase shift is parameterized as

$$q \cot \delta_{0+}^{3/2} = (a_{0+}^{3/2})^{-1} + b_3\epsilon + c_3\epsilon^2, \quad (1)$$

where  $q$  denotes (the magnitude of) the CM 3-momentum. The  $p_{1/2}$ -wave phase shift is parameterized according to the form

$$\tan \delta_{1-}^{3/2}/q = d_{31}\epsilon + e_{31}\epsilon^2. \quad (2)$$

Since the  $p_{3/2}$  wave contains the  $\Delta(1232)$  resonance, a singular (at  $W = m_\Delta$ ) term must be added to the background term, leading to the expression

$$\tan \delta_{1+}^{3/2}/q = d_{33}\epsilon + e_{33}\epsilon^2 + \frac{\Gamma_\Delta m_\Delta}{2q_\Delta^3(p_{0\Delta} + m_p)} \frac{(p_0 + m_p)q^2}{W(m_\Delta - W)}, \quad (3)$$

where  $\Gamma_\Delta$  is the  $\Delta(1232)$  width,  $m_\Delta$  is the  $\Delta(1232)$  mass,  $m_p$  is the proton mass,  $p_0$  is the proton CM energy, and  $W$  is the total CM energy. The quantities  $q_\Delta$  and  $p_{0\Delta}$  denote the values of the variables  $q$  and  $p_0$ , respectively, at the position of the  $\Delta(1232)$  resonance ( $W = m_\Delta$ ). The singular term in Eq. (3)

has been obtained from Ref. [6], see  $K_{1+}$  in Eqs. (39) and the corresponding  $K_{1+}^{3/2}$  element (after the isospin decomposition of  $K_{1+}$  is taken into account), as well as footnote 10 therein.

### 2.1.2 Fits to our low-energy $\pi^-p$ elastic-scattering and charge-exchange databases using the $K$ -matrix parameterizations

The isospin  $I = 3/2$  amplitudes, obtained in the final fit to the truncated low-energy  $\pi^+p$  DB (i.e., to the DB obtained after the removal of the outliers) using the  $K$ -matrix parameterizations of the preceding section, are imported into the analysis of low-energy  $\pi^-p$  ES and CX DBs. In this part, another seven parameters (different for these two DBs) are introduced, to parameterize the  $I = 1/2$  amplitudes. The new parametric forms are similar to those given by Eqs. (1-3), with the parameters  $a_{0+}^{1/2}$ ,  $b_1$ ,  $c_1$ ,  $d_{13}$ ,  $e_{13}$ ,  $d_{11}$ , and  $e_{11}$ . Of course, it is necessary to explicitly include the contribution of the Roper resonance  $N(1440)$  in  $\delta_{1-}^{1/2}$ :

$$\tan \delta_{1-}^{1/2}/q = d_{11}\epsilon + e_{11}\epsilon^2 + \frac{\Gamma_R M_R (p_{0R} + m_p)}{2q_R^3 (M_R + m_p)^2} \frac{(W + m_p)^2 q^2}{W(M_R - W)(p_0 + m_p)} \quad , \quad (4)$$

where (as we are dealing with energies below the pion-production threshold)  $\Gamma_R$  is the partial width of the Roper resonance to  $\pi N$  decay modes and  $m_R$  is its mass. The quantities  $q_R$  and  $p_{0R}$  denote the  $q$  and  $p_0$  values at the resonance position ( $W = M_R$ ). The singular term in Eq. (4) has been obtained from Ref. [6], see Section 3.5.1 therein, in particular, Eq. (54) for  $K_{1-}$ .

## 2.2 Minimization function

In our recent partial-wave analyses (PWAs) of the  $\pi N$  data, we make use of the minimization function given by the Arndt-Roper formula [2], i.e., of the minimization function which the SAID group also use in their analyses. The contribution of the  $j$ -th data set to the overall  $\chi^2$  is of the form:

$$\chi_j^2 = \sum_{i=1}^{N_j} \left( \frac{z_j y_{ij}^{\text{th}} - y_{ij}^{\text{exp}}}{\delta y_{ij}^{\text{exp}}} \right)^2 + \left( \frac{z_j - 1}{\delta z_j} \right)^2 \quad , \quad (5)$$

where  $y_{ij}^{\text{exp}}$  denotes the  $i$ -th data point of the  $j$ -th data set,  $y_{ij}^{\text{th}}$  the corresponding fitted (‘theoretical’) value,  $\delta y_{ij}^{\text{exp}}$  the statistical uncertainty of the  $y_{ij}^{\text{exp}}$  data point,  $z_j$  a scale factor applied to the entire data set,  $\delta z_j$  the normalization uncertainty (reported by the experimental group or assigned by us), and  $N_j$  the number of the data points in the data set after the removal of any outliers. The fitted values  $y_{ij}^{\text{th}}$  are obtained by means of the parameterized forms of the  $s$ - and  $p$ -wave amplitudes detailed in Sections 2.1.1 and 2.1.2. The values of

the scale factor  $z_j$  are determined (separately for each data set) in such a way as to minimize  $\chi_j^2$ . For each data set, a unique solution for  $z_j$  is obtained via the relation:

$$z_j = \frac{\sum_{i=1}^{N_j} y_{ij}^{\text{th}} y_{ij}^{\text{exp}} / (\delta y_{ij}^{\text{exp}})^2 + (\delta z_j)^{-2}}{\sum_{i=1}^{N_j} (y_{ij}^{\text{th}} / \delta y_{ij}^{\text{exp}})^2 + (\delta z_j)^{-2}} , \quad (6)$$

which leads to

$$(\chi_j^2)_{\min} = \sum_{i=1}^{N_j} \frac{(y_{ij}^{\text{th}} - y_{ij}^{\text{exp}})^2}{(\delta y_{ij}^{\text{exp}})^2} - \frac{\left( \sum_{i=1}^{N_j} y_{ij}^{\text{th}} (y_{ij}^{\text{th}} - y_{ij}^{\text{exp}}) / (\delta y_{ij}^{\text{exp}})^2 \right)^2}{\sum_{i=1}^{N_j} (y_{ij}^{\text{th}} / \delta y_{ij}^{\text{exp}})^2 + (\delta z_j)^{-2}} . \quad (7)$$

The overall  $\chi^2 = \sum_{j=1}^N (\chi_j^2)_{\min}$  (where  $N$  denotes the number of the accepted data sets in the fit) is a function of the parameters entering the modeling of the  $s$ - and  $p$ -wave amplitudes. These parameters are varied until  $\chi^2$  attains its minimal value  $\chi_{\min}^2$ .

The part of  $(\chi_j^2)_{\min}$  which represents the pure random fluctuation in the measurements of the  $j$ -th data set (i.e., the ‘unexplained variation’ in standard regression terminology) may be obtained from Eq. (7) in the limit  $\delta z_j \rightarrow \infty$ , which is equivalent to removing the term  $(\delta z_j)^{-2}$  from the denominator of the second term on the right-hand side (rhs) of the expression; we denote this value by  $(\chi_j^2)_{st}$ . The variation which is contained in  $(\chi_j^2)_{\min}$  in excess of  $(\chi_j^2)_{st}$  is associated with the contribution from the floating (rescaling) of the data set. The expression for  $(\chi_j^2)_{sc} \equiv (\chi_j^2)_{\min} - (\chi_j^2)_{st}$  is

$$(\chi_j^2)_{sc} = \frac{(\delta z_j)^{-2} \left( \sum_{i=1}^{N_j} y_{ij}^{\text{th}} (y_{ij}^{\text{th}} - y_{ij}^{\text{exp}}) / (\delta y_{ij}^{\text{exp}})^2 \right)^2}{\sum_{i=1}^{N_j} (y_{ij}^{\text{th}} / \delta y_{ij}^{\text{exp}})^2 \left( \sum_{i=1}^{N_j} (y_{ij}^{\text{th}} / \delta y_{ij}^{\text{exp}})^2 + (\delta z_j)^{-2} \right)} . \quad (8)$$

The scale factors which minimize only the first term on the rhs of Eq. (5) are obtained from Eq. (6) in the limit  $\delta z_j \rightarrow \infty$ :

$$\hat{z}_j = \frac{\sum_{i=1}^{N_j} y_{ij}^{\text{th}} y_{ij}^{\text{exp}} / (\delta y_{ij}^{\text{exp}})^2}{\sum_{i=1}^{N_j} (y_{ij}^{\text{th}} / \delta y_{ij}^{\text{exp}})^2} . \quad (9)$$

The scale factors  $\hat{z}_j$  represent the optimal floating of the fitted values  $y_{ij}^{\text{th}}$  around the experimental results  $y_{ij}^{\text{exp}}$ , with no regard to the normalization uncertainty.

The analysis of this work may be performed using either of the two scale factors,  $z_j$  or  $\hat{z}_j$ . We make use of the scale factors  $z_j$ , as only these quantities are contained in the output of the SAID Analysis Program.

For the purpose of the optimization, we employ the standard MINUIT package [7] of the CERN library (FORTRAN version). Each optimization has been achieved on the basis of the (robust) SIMPLEX-MINIMIZE-MIGRAD-MINOS sequence. All fits of this work terminated successfully.

### 3 Results from our partial-wave analysis

The list of the experiments, which are included in our three  $\pi N$  DBs, is available from Refs. [5,8]; the same notation will be used here to identify the individual data sets. Our DBs contain differential cross sections (DCSs), analyzing powers (APs), partial-total cross sections (PTCSs), and total (as well as total-nuclear) cross sections (TCSs) for  $T \leq 100$  MeV. The largest difference between the SAID DB for  $T \leq 100$  MeV and ours relates to the ES DCSs of the CHAOS Collaboration [9,10]. Regarding these measurements, our opinion is known [11,12] and there is no reason to repeat it here.

Modifications in the analysis software and DB structure in the recent years enable us now to also include in the optimization the APs of Ref. [13], comprising a total of 28 data points. There had been two technical reasons preventing the direct use of these measurements in our PWAs before 2013: a) each of the three data sets, to which the measurements of Ref. [13] must be assigned, involves more beam energies than one and b) the last of these data sets contains measurements of both ES reactions.

Regarding the proton EM form factors, recent developments suggest the replacement of the forms we had been using before 2013. The parameterization of the Dirac  $F_1^p(t)$  and Pauli  $F_2^p(t)$  form factors of the proton with (traditional) dipole forms has been found to provide a poor description of the ‘world’ electron-proton ( $ep$ ) unpolarized and polarized data [14]. Although the sensitivity of our results to the details of the parameterization of these quantities is low (due to the smallness of the  $Q^2$  transfer for  $T \leq 100$  MeV), adopted now is an improved parameterization. In Ref. [15], the authors made use of the so-called Padé parameterization [16] for the Sachs EM form factors  $G_E^p(t)$  and  $G_M^p(t)$  (the superscript  $p$  is omitted in Ref. [15]), and obtained the optimal values of the relevant parameters from a fit to  $ep$  measurements; we now use the results of their Table II. The pion form factor  $F^\pi(t)$  is usually parameterized via a monopole form, e.g., see Ref. [17]. Although results of the same quality are obtained in the low-energy region with either a monopole or a dipole form, the monopole parameterization is now adopted.

The values of the relevant physical constants (see Table 1) have been fixed from the 2014 compilation of the Particle-Data Group (PDG) [18]. Finally, an improved approach for determining the (small)  $d$  and  $f$  waves has been implemented; to suppress artefacts which are due to the truncation of small values, simple polynomials are now fitted to the  $d$ - and  $f$ -wave phase shifts of the SAID analysis [1], which (as it incorporates dispersion-relation constraints) is expected to determine reliably these phase shifts in the region  $T > 100$  MeV.

One statistical test for each data set is performed, the one involving its con-

tribution  $(\chi_j^2)_{\min}$  to the overall  $\chi_{\min}^2$  (see Section 2.2). The p-value, estimated from  $(\chi_j^2)_{\min}$  and  $N_j$ , is compared to the user-defined confidence level  $p_{\min}$  for the acceptance of the null hypothesis (no statistically significant effects); in case that the extracted p-value is below  $p_{\min}$ , the degree of freedom (DOF) with the largest contribution to  $(\chi_j^2)_{\min}$  is eliminated in the subsequent fit. As in our recent PWAs, we adopt the  $p_{\min}$  value which is associated with a  $2.5\sigma$  effect in the normal distribution. This value is approximately equal to  $1.24 \cdot 10^{-2}$ , i.e., slightly larger than  $1.00 \cdot 10^{-2}$ , a threshold which most statisticians recommend as the outset of statistical significance.

When identifying the outliers in our past PWAs, the maximal number of excluded data points for each data set had been fixed (somewhat arbitrarily) at 2; data sets with more excluded DOFs were removed from the analysis. To do justice to data sets containing a large number of data points, this restriction was recently revised<sup>2</sup>. Assuming pure statistical fluctuation, the probability that the  $j$ -th data set contains at most 2 outliers decreases with increasing  $N_j$  values. Evidently, the maximal number of outliers must be determined separately for each data set, on the basis of the number of measurements which the data set initially contains.

Let us assume that the *a-priori* probability for a data point to be an outlier is equal to  $p$ . The probability that the  $j$ -th data set (with  $N_j$  initial data points) contains exactly  $k$  outliers is then given by the expression

$$P_k = \binom{N_j}{k} p^k (1-p)^{N_j-k} . \quad (10)$$

Consequently, the probability that the  $j$ -th data set contains up to  $N_j^{\text{out}} \leq N_j$  outliers is given by the sum

$$P(N_j^{\text{out}}) = \sum_{k=0}^{N_j^{\text{out}}} P_k . \quad (11)$$

After  $p_{\min}$  is set, the maximal number of outliers permitted for the particular experiment (at that  $p_{\min}$  level) may be identified as the maximal  $N_j^{\text{out}}$  value for which the cumulative probability, obtained with Eq. (11), does not exceed  $1 - p_{\min}$ . It thus follows that, if  $p = 0.06$ , a data set with 20 data points will be allowed to contain 3 outliers, whereas one with only 10 data points a maximum of 2 outliers for the  $p_{\min}$  value adopted herein. To obtain an estimate of  $p$ , the maximal number of outliers  $N_j^{\text{out}}$  was set equal to  $N_j$  (which is equivalent to relaxing the condition for removing entire data sets) and the fits to our low-energy  $\pi^+p$  DB (which is known to contain the largest proportion of outliers) were carried out iteratively, excluding at each iteration step the data point with

---

<sup>2</sup> This modification does not affect any of the results we have obtained thus far for  $p_{\min} \approx 1.24 \cdot 10^{-2}$ .

the largest contribution to the overall  $\chi^2_{\min}$ . The procedure was repeated until no data point could be identified as an outlier. An estimate of the probability  $p$  is obtained as the fraction of the number of DOFs (NDF) of the initial  $\pi^+p$  DB which had to be eliminated. To avoid the exclusion of low- $N_j$  data sets just because of the removal of 1 DOF,  $N_j^{\text{out}}$  was finally redefined as  $\max\{N_j^{\text{out}}, 2\}$ .

Data sets which do not give acceptable  $p$ -values (i.e., exceeding  $p_{\min}$ ) after the elimination of the appropriate number of data points (the absolute normalization is also considered to be one of the acquired measurements), as explained above, were removed from the DB. Only one point was removed at each step. The optimization was repeated, until no data point could be identified as an outlier. It must be emphasized that, in our approach, the identification of the outliers in each of the three reactions is based on comparisons involving *only* the measurements in that particular reaction.

### 3.1 Fits to our low-energy $\pi^+p$ database

Our initial low-energy  $\pi^+p$  DB contains 57 data sets consisting of 389 data points. As in all our past PWAs, we found that the data sets of BRACK90 at 66.80 MeV and JORAM95 at 32.70 MeV (with 11 and 7 data points, respectively) had to be removed from the DB. Subsequently, three data sets had to be freely floated, namely two of the BRACK86 data sets (at 66.80 and 86.80 MeV), as well as the BRACK90 data set at 30.00 MeV. Three additional single data points had to be removed. After the elimination of 24 DOFs of the initial DB, we obtained a truncated low-energy  $\pi^+p$  DB comprising 55 data sets and 365 DOFs. The accepted data sets are detailed in Table 2.

The  $\chi^2_{\min}$  value, corresponding to the fit to the initial DB, was 706.7; for the truncated DB,  $\chi^2_{\min} \approx 459.5$ . Therefore, the removal of 24 DOFs from the initial DB results in the decrease of the  $\chi^2$  by 247.2 units, corresponding to more than 10 units per removed entry on average. At the same time, the  $p$ -value of the fit increased by over 17 orders of magnitude.

The scale factors  $z_j$ , corresponding to the DCSs in our low-energy  $\pi^+p$  DB <sup>3</sup>, are shown in Fig. 1. The weighted linear fit to the data shown (the weight of each entry is equal to  $(\delta z_j)^{-2}$ ) yields an intercept of  $1.023 \pm 0.033$  and a slope of  $(-0.38 \pm 0.40) \cdot 10^{-3} \text{ MeV}^{-1}$ ; both fitted values are compatible with the expectation values (of 1 and 0, respectively) for a successful optimization.

---

<sup>3</sup> Being ratios of cross sections, the APs are not suitable for the demonstration of the systematic effects which we have set about investigating in this study. The PTCSSs and the TCSs (all one- or two-point data sets) have been used in the optimization, but have not been included in the analysis of the scale factors shown in Fig. 1, as the SAID group do not include these measurements in their DB.

It is sometimes suggested that the joint analysis of the DCSs and the PTCSs in the  $\pi^+p$  reaction may be inappropriate, as the integrated DCS might not match the measured PTCS. Such a mismatch could be due to the effects of a presently unknown state characterized by a  $\pi N$  decay mode, e.g., as the case would be if a  $\pi N$  resonance, not currently established, existed below the  $\Delta(1232)$  mass (see also Section 6). We have investigated the sensitivity of our results to the inclusion of the PTCSs/TCSs in the fitted  $\pi^+p$  DB and have concluded that our analysis is very little affected by the treatment of these measurements. To demonstrate this, we also mention the fitted values of the intercept and of the slope after the  $\pi^+p$  PTCSs/TCSs are removed from the input DB: the new intercept comes out equal to  $1.025 \pm 0.028$ , whereas the new slope is  $(-0.31 \pm 0.36) \cdot 10^{-3} \text{ MeV}^{-1}$ . We performed this check only for the sake of completeness, with no intention to cast doubt on the validity of the low-energy  $\pi^+p$  PTCSs/TCSs. In our approach, we have found no evidence of mismatch between the DCSs and the PTCSs/TCSs: these two observables can be accounted for in a joint optimisation scheme.

### 3.2 *Fits to our low-energy $\pi^-p$ elastic-scattering database*

Our initial low-energy  $\pi^-p$  ES DB contains 37 data sets consisting of 339 data points. The BRACK90 data set at 66.80 MeV (with 5 data points in total) needed to be removed, one data set (the WIEDNER89 data set at 54.30 MeV) had to be freely floated, and two additional single data points had to be removed. After the elimination of 8 DOFs of the initial DB, we obtained a truncated low-energy  $\pi^-p$  ES DB comprising 36 data sets and 331 DOFs. The accepted data sets are detailed in Table 3.

The  $\chi^2_{\min}$  value, corresponding to the fit to the initial DB, was 524.8; for the truncated DB,  $\chi^2_{\min} \approx 371.0$ . Therefore, the removal of only 8 DOFs from the initial DB results in a decrease of the  $\chi^2$  by 153.8 units, i.e., just short of 20 units per removed entry on average. At the same time, the p-value of the fit increased by over 8 orders of magnitude.

The scale factors  $z_j$ , corresponding to the DCSs in our low-energy  $\pi^-p$  ES DB, are shown in Fig. 2. The weighted linear fit to the data shown yields an intercept of  $1.007 \pm 0.019$  and a slope of  $(-0.08 \pm 0.24) \cdot 10^{-3} \text{ MeV}^{-1}$ ; both fitted values are compatible with the expectation for a successful optimization.

### 3.3 *Fits to our low-energy $\pi^-p$ charge-exchange database*

Our initial low-energy  $\pi^-p$  CX DB contains 54 data sets consisting of 333 data points. Only 5 DOFs needed to be removed: the FITZGERALD86 data

sets at 32.48, 36.11, 40.26, and 47.93 MeV needed to be freely floated, and the BREITSCHOPF06 TCS at 75.10 MeV had to be removed. After the elimination of these 5 DOFs of the initial DB, we obtained a truncated low-energy  $\pi^-p$  CX DB comprising 53 data sets and 328 DOFs. The accepted data sets are detailed in Table 4.

The  $\chi_{\min}^2$  value, corresponding to the fit to the initial DB, was 401.6; for the truncated DB,  $\chi_{\min}^2 \approx 313.7$ . Therefore, the removal of only 5 DOFs from the initial DB results in a decrease of the  $\chi^2$  by 87.9 units, i.e., to 17.6 units per removed entry on average.

The scale factors  $z_j$ , corresponding to the DCSs in our low-energy  $\pi^-p$  CX DB, are shown in Fig. 3. The weighted linear fit to the data shown yields an intercept of  $1.002 \pm 0.015$  and a slope of  $(0.05 \pm 0.27) \cdot 10^{-3} \text{ MeV}^{-1}$ ; again, both fitted values are compatible with the expectation for a successful optimization.

## 4 Results from the WI08 solution

The SAID  $\pi^+p$  DB for  $T \leq 100$  MeV contains 721 data points, 679 of which relate to DCSs, the remaining 42 to APs; PTCSs and TCSs are not included. The DB contains the entirety of the DENZ05 data, as well as the BERTIN76 measurements (save for the 67.40 MeV data set). The BERTIN76, the AULD79, and the FRANK83 data sets are floated <sup>4</sup>. The overall  $\chi_{\min}^2$ , corresponding to the SAID  $\pi^+p$  DB for  $T \leq 100$  MeV, is equal to 1595.2, yielding a p-value of a few  $10^{-68}$ . Evidently, the description of the SAID  $\pi^+p$  DB for  $T \leq 100$  MeV with the WI08 phase-shift solution is poor.

The SAID  $\pi^-p$  ES DB for  $T \leq 100$  MeV contains 634 data points, 546 of which relate to DCSs, the remaining 88 to APs. Similar to us (but for different reasons <sup>5</sup>), they have not included the corresponding PTCSs and TCSs in their DB. Their DB contains the entirety of the DENZ05 data. The four FRANK83 data sets are floated. The overall  $\chi_{\min}^2$ , corresponding to the SAID  $\pi^-p$  ES DB for  $T \leq 100$  MeV, is equal to 1102.1, yielding a p-value of about  $10^{-27}$ .

---

<sup>4</sup> The definition of floating for the SAID group is not identical to ours. For us, free floating involves the limit  $\delta z_j \rightarrow \infty$ , whereas they simply set the corresponding normalization uncertainty  $\delta z_j$  of the data set to the value of 1. This value drastically reduces, but does not eliminate, the contribution of the floating contribution  $(\chi_j^2)_{sc}$  of Eq. (8) to  $(\chi_j^2)_{\min}$  of Eq. (7).

<sup>5</sup> Given that the nine available  $\pi^-p$  PTCSs and TCSs contain a component from CX scattering, these measurements have never been included in our  $\pi^-p$  ES DB. Their involvement in any part of the analysis (see beginning of Section 5) would complicate the discussion on the violation of the isospin invariance in the  $\pi N$  interaction.

Therefore, the description of the SAID  $\pi^-p$  ES DB for  $T \leq 100$  MeV with the WI08 solution is almost as poor as that of their  $\pi^+p$  DB.

The SAID  $\pi^-p$  CX DB for  $T \leq 100$  MeV contains 353 data points, 343 of which relate to DCSs, the remaining 10 to APs; the corresponding TCSs are not included therein. The three DUCLOS73 measurements have been deleted from their DB. The overall  $\chi^2_{\min}$ , corresponding to the SAID  $\pi^-p$  CX DB for  $T \leq 100$  MeV, is equal to 401.3, yielding a p-value of about  $3.9 \cdot 10^{-2}$ . The description of the SAID  $\pi^-p$  CX DB for  $T \leq 100$  MeV with the WI08 solution is acceptable.

There are three reasons why the description of *their* low-energy ES DBs with *their* WI08 solution is poor.

- The SAID  $\pi N$  DB is very extensive. The low-energy behavior of the partial-wave amplitudes is largely determined from measurements acquired at higher energies. As the total amount of the measurements, contained in their DB, exceeds 50 000 data points, their 1 708 low-energy measurements are literally swamped in the analysis.
- The SAID group include in their DBs all the available measurements (including a few data sets which have not appeared in formal publications); outliers are seldom excluded.
- The three  $\pi N$  reactions are subject to an analysis which assumes the fulfillment of the isospin invariance in the  $\pi N$  interaction at all energies.

We will now report the results of a very simple analysis of the scale factors  $z_j$  for  $T \leq 100$  MeV, as these quantities come out of their fits to the data. These values (two decimal digits are available online) were obtained from the SAID web page on May 6, 2016; we also use their  $T_j$  and  $\delta z_j$  values. Scatter plots of the scale factors  $z_j$  versus the corresponding beam energy  $T_j$  for the data sets of the SAID DB are shown, *separately* for the three  $\pi N$  reactions, in Figs. 4-6. The fitted values of the parameters of the weighted linear fits (as well as their uncertainties, corrected with the Birge factor  $\sqrt{\chi^2/\text{NDF}}$ ), are shown in Table 5. Visual inspection of these figures and of Table 5 leads to two conclusions:

- In all three  $\pi N$  reactions, the departure of the scale factors  $z_j$  from the expectation for a successful optimization is noticeable. The energy dependence of the scale factors  $z_j$  is more pronounced in the case of the  $\pi^+p$  reaction.
- The departure from the expectations appears to occur slightly below  $T = 100$  MeV; decreasing effects with increasing beam energy are observed.

If the scale factors from the three  $\pi N$  reactions are analyzed in a joint scheme, then the systematic effects, observed in the individual reactions, disappear. This becomes evident after comparing the last row of Table 5 with the previous three, as well as after comparing Fig. 7 with Figs. 4-6.

## 5 Similarities and differences between the two approaches

In our method of extracting the important information from the  $\pi N$  measurements for  $T \leq 100$  MeV, three steps are followed. At the first step, we employ simple parameterizations of the  $s$ - and  $p$ -wave  $K$ -matrix elements, retaining in the expressions orders up to  $\epsilon^2$ . We make use of these general parameterizations in order to reliably identify and remove any outliers present in the initial DBs, thus obtaining self-consistent input for the subsequent phases of the analysis. At the second step of our approach, the ETH model of the  $\pi N$  interaction (a complete description of this model and details on its development may be found in Ref. [6]) is fitted to the truncated DBs of the two ES reactions, thus leading to the determination of the values of the model parameters (coupling constants and vertex factors), which account optimally for the measurements of these two reactions. At a third step, we investigate the violation of the isospin invariance in the  $\pi N$  interaction, by comparing the model predictions for the CX reaction (obtained from the fitted values, as well as the correlation matrix of the fit to the two ES DBs) to the measurements of the CX reaction. We reported in the past that these predictions significantly *underestimate* the CX DCSs in most of the low-energy region. Assuming the correctness of the bulk of the available measurements and the smallness of any missing pieces in the EM corrections, this mismatch between predictions and measurements strongly indicates the violation of the isospin invariance in the  $\pi N$  interaction at low energy (for a more detailed discussion, see Section 7 of Ref. [5]). Following a slightly different methodology (and fewer CX measurements), Gibbs, Ai, and Kaufmann came to the same conclusion in the mid 1990s [3].

Our PWAs are restricted to  $T \leq 100$  MeV, because the ETH model is expected to work better in the low-energy region and because our EM corrections [19,20] have been established only below 100 MeV. Regarding the former remark, the introduction of strong-interaction form factors in the Feynman graphs of the ETH model is unnecessary below 100 MeV and the contributions from graphs involving distant baryonic states - i.e., the higher baryon resonances with masses above 2 GeV - to the  $s$ - and  $p$ -wave amplitudes of the model are expected to be negligible.

A dispersion-relation analysis framework, such as the one developed by the SAID group, assumes the fulfillment of the isospin invariance in the  $\pi N$  interaction and analyzes the entire DB available, extending to  $T$  values of several GeV, so that the dispersion integrals be evaluated reliably. Such an approach cannot be performed in a restricted energy region, without bringing in external influences. Such a framework cannot be used in order to conduct exclusive analyses of the data, be they restricted in energy or involving only one reaction. This is one important difference between our approach and theirs. The second

difference relates to the procedure: we choose to analyze the two ES processes (this analysis fixes the  $I = 3/2$  and  $I = 1/2$  amplitudes) and subsequently investigate whether isospin invariance is fulfilled in the  $\pi N$  interaction, on the basis of comparisons with the measurements of the third reaction (triangle identity <sup>6</sup>). On the contrary, the SAID group assume the fulfillment of the isospin invariance in the  $\pi N$  interaction at all energies, and analyze the three  $\pi N$  reactions in a joint optimization scheme.

So far, the emphasis has been placed on the differences between the two approaches. However, there are also similarities. For instance, both approaches rely on the correctness of the input data. To an extent, we take steps towards investigating the self-consistency of the input DB, whereas they avoid excluding measurements. Only considering the number of the input data points, the sensitivity of our analysis to outliers is expected to be more pronounced than it is in their case: 500 discrepant DCSs in a DB of 1 000 data points wreck havoc; the same amount of discrepant measurements in a DB of over 50 000 data points is surely less problematic. As a result, we cannot but thoroughly examine every new data set prior to including it in the DB; in this respect, they can afford to be more generous. Finally, both approaches rely on the correctness/completeness of the method incorporating the EM effects (distortion corrections to the hadronic phase shifts and to the partial-wave amplitudes) in the analysis.

To summarize, the SAID group assume that isospin invariance in the  $\pi N$  interaction is fulfilled at all energies, whereas we test whether it is at low energy. They cannot easily restrict their analysis to specific energy regions or reactions, whereas we may perform a variety of analyses in relation to the input DBs: we may perform joint analyses (e.g., by using as input the  $\pi^+ p$  DB along with either of the  $\pi^- p$  DBs or by submitting the measurements of all three  $\pi N$  reactions to a joint optimization scheme) or we may analyze the three  $\pi N$  reactions independently of one another (using our  $K$ -matrix parameterizations). However, our analyses can only involve the low-energy region. Both approaches rely on the correctness of the bulk of the measurements (ours is significantly more sensitive to the presence of outliers in the DB) and both approaches rely on the correctness of the EM corrections, applied to the hadronic phase shifts and to the partial-wave amplitudes on the way to fitting the observables.

---

<sup>6</sup> Assuming that the isospin invariance holds in the  $\pi N$  interaction, only two (of course, complex) amplitudes enter the physical description of the three  $\pi N$  reactions: the  $I = 3/2$  amplitude ( $f_3$ ) and the  $I = 1/2$  amplitude ( $f_1$ ). Disregarding the distortions which are due to the EM effects, the  $\pi^+ p$  reaction is described by  $f_3$ , the  $\pi^- p$  ES reaction by  $(2f_1 + f_3)/3$ , and the CX reaction by  $\sqrt{2}(f_3 - f_1)/3$ . On the basis of these relations, the triangle identity between the three corresponding amplitudes  $f_{\pi^+ p}$ ,  $f_{\pi^- p}$ , and  $f_{CX}$  is obtained:  $f_{\pi^+ p} - f_{\pi^- p} = \sqrt{2}f_{CX}$ .

## 6 Discussion and conclusions

A self-consistent,  $\chi^2$ -based optimization scheme satisfies the requirement that the distribution of the normalized residuals of the fit follow the  $N(0, 1)$  distribution. Furthermore, these residuals must not exhibit significant dependence on the independent variables in the problem, e.g., on the beam energy in this work. In a self-consistent optimization scheme, where the input measurements are reliable and their modeling adequate, all fluctuations present in the residuals are random. We demonstrated that the results of the weighted linear fits to the scale factors  $z_j$ , obtained from the data when using our  $K$ -matrix parameterizations, come out as expected: independent of the beam energy and ‘clustering’ around the expectation value of 1 (see Figs. 1-3).

The SAID analysis rests upon the fulfillment of three conditions *at all energies*:

- (a) that the bulk of the experimental data is reliable;
- (b) that the EM effects are correctly accounted for; and
- (c) that the isospin invariance is fulfilled in the  $\pi N$  interaction.

When the Arndt-Roper formula is used in the optimization, one expects that the data sets which must be scaled ‘upwards’ should be balanced (on average) by those which must be scaled ‘downwards’. Additionally, the energy dependence of the scale factors must not be significant. If these prerequisites are not fulfilled, the modeling of the input measurements cannot be considered to be satisfactory. The scale factors, relating to the description of the SAID low-energy  $\pi N$  DBs with the WI08 solution, are shown in Fig. 7. At first glance, the plot leaves a satisfactory impression, in particular after considering the extent of the SAID  $\pi N$  DB, as well as the practice of the SAID group to avoid excluding the outliers. Consequently, the optimization scheme leading to the WI08 solution yields normalized residuals for the scale factors <sup>7</sup> which are reasonably well centered on 0 (we disregard small effects). Given that the reduced  $\chi^2$ , corresponding to the entirety of the fitted data at low energy in the case of the WI08 solution, is about 1.81, the joint analysis of the data inevitably yields normalized residuals with a distribution broader than the  $N(0, 1)$  distribution. However, this broadening originates in the choice of the SAID group to seldom exclude outliers.

Let us finally express our criticism on the low-energy behavior of the WI08 solution. The SAID input DB consists of three distinct parts, identified as the sets of measurements of the three  $\pi N$  reactions. Had their fit been unbiased, the general behavior of the fitted  $z_j$  values in terms of their dependence on  $T_j$ , as obtained from Fig. 7, would also have been observed in any arbitrary subset of their DB, consistent with the basic principles of the Sampling Theory

---

<sup>7</sup> These residuals are equal to  $(z_j - 1)/\delta z_j$ , see Eq. (5).

(adequate population, representative sampling). The scale factors, relating to the description of the SAID low-energy  $\pi N$  DBs with the WI08 solution, are shown (separately for the three reactions) in Figs. 4-6. Had the three aforementioned conditions (a)-(c) been fulfilled in the SAID analysis at all energies, the scale factors of Figs. 4-6 would have come out independent of the beam energy and would have been centered on 1, as the case was for the joint analysis of Fig. 7. However, the bulk of the data for  $T \leq 100$  MeV (represented by the shaded bands in Figs. 4-6) appears to be either underestimated by the WI08 solution (i.e., in case of the CX reaction) or overestimated by it (i.e., in case of the two ES reactions, the effects for the  $\pi^+p$  reaction being more pronounced). One notices that the mismatches decrease with increasing beam energy, converging to  $z = 1$  in the vicinity of  $T = 100$  MeV. Such a behavior is consistent with the general conclusions of Refs. [3,4,5] for an energy-dependent isospin-breaking effect.

Of course, the question arises whether the departure from the triangle identity is indicative of missing features in the physical description of the  $\pi N$  interaction at low energy. For instance, the assumption has always been that the  $\pi^+p$  interaction at low energy is purely elastic and that all the inelasticity corrections, applied to the amplitudes and to the phase shifts, are (small and) known [21,22,23]. On the other hand, the speculation is frequently voiced that the mismatches, observed on several occasions in the low-energy  $\pi N$  interaction (in particular, in the  $\pi^+p$  reaction), could be attributed to the incompleteness of the currently used theoretical background, rather than to experimental discrepancies. For instance, such a scenario could be possible if a (broad)  $\pi N$  resonance existed below the  $\Delta(1232)$  mass; at present, no such state has been detected. Far-fetched as this possibility might appear at first glance, it may be equally difficult to either refute or endorse it.

From Figs. 4-6 and from Table 5, one may conclude that the WI08 solution does not describe sufficiently well the bulk of the low-energy measurements in any of the three  $\pi N$  reactions. Evidently, the WI08 solution at low energy represents a fictitious, average  $\pi N$  process, one which does not adequately capture the dynamics of the three physical  $\pi N$  reactions. Regarding the analysis of the scale factors obtained with the WI08 solution, we stress (once again) that herein we have only fitted straight lines to their  $z_j$  values, as they appear in the SAID web page [1]; we have used no input from our approach when analyzing their  $z_j$  values.

The conclusion appears to be inevitable. Even in a framework of an analysis assuming the isospin invariance (as the case is for the WI08 solution), the isospin-breaking effects, albeit somewhat hidden, manifest themselves as systematic trends in the output of the optimization and may be uncovered if the three  $\pi N$  reactions are analyzed *separately*. This conclusion strengthens our argument on investigating the behavior of the normalized residuals in PWAs

of the low-energy measurements.

One might argue that the effects, contained in Figs. 4-6 and in Table 5, are not ‘large’. However, it must be borne in mind that the isospin-breaking effects in the  $\pi N$  domain are not expected to be large. Gibbs, Ai, and Kaufmann [3] have shown that such effects mainly affect the  $s$ -wave part of the amplitude (10% effects are seen in their Fig. 1), and (to a lesser extent) the no-spin-flip  $p$ -wave part (smaller effects are seen in their Figs. 2). We have shown that the largest departure from the isospin invariance occurs in the phase shifts  $\delta_{0+}^{1/2}$  and  $\delta_{1+}^{3/2}$ , see Figs. 2 and 3 of Ref. [5]. Both analyses appear to agree on the expected magnitude of such effects: roughly speaking, effects between 5 and 10% (in the amplitude) are expected at low energy. The systematic effects, observed in Figs. 4-6 of this work, have about the right size, as well as an energy dependence which is consistent with the findings of Refs. [3,4,5].

To conclude, we briefly compare the level of the violation of the isospin invariance in the  $\pi N$  interaction [3,4,5] with what has long been known for the  $NN$  system [24]. The hadronic part of the low-energy  $NN$  interaction is characterized by three scattering lengths, corresponding to the three  $^1S_0$  states  $pp$ ,  $nn$ , and  $np$ . If charge independence (which is used in the  $NN$  domain as a synonym for isospin invariance) would hold, these three scattering lengths would be equal. In fact, the values obtained after the EM effects are removed are [24]:

$$a_{pp} = -17.3(4) \text{ fm}, \quad a_{nn} = -18.8(3) \text{ fm}, \quad a_{np} = -23.77(9) \text{ fm} . \quad (12)$$

(In Ref. [24], the three scattering lengths carry the superscript ‘N’, indicating that these quantities are nuclear ones, i.e., obtained after the EM corrections have been made.) Obviously, these numbers violate charge independence and, to a lesser extent, charge symmetry, as

$$\Delta a_{CD} = (a_{pp} + a_{nn})/2 - a_{np} = 5.7(3) \text{ fm} \quad (13)$$

and

$$\Delta a_{CSD} = a_{pp} - a_{nn} = 1.5(5) \text{ fm} \quad (14)$$

are significantly non-zero. This corresponds to a violation of the charge independence in the low-energy  $NN$  interaction around 27% and of charge symmetry about 8%. The level of the charge-independence breaking in the  $NN$  interaction is to be compared with the 5 to 10% effects which have been reported in Refs. [3,4,5] for the low-energy  $\pi N$  system. If the  $\pi N$  interaction is regarded as the ‘fundamental’ element for the description of the  $NN$  interaction (as the case is in the framework of the meson-exchange theories of the strong interaction), it is logical to expect that the isospin-breaking effects cascade from the  $NN$  interaction down to the  $\pi N$  interaction. Under the assumption that the nuclear force in the  $NN$  interaction is modeled at

low energy via the one-pion exchange mechanism, Babenko and Petrov [25] recently obtained a considerable splitting of the  $\pi N$  coupling constant, i.e., significantly different values for the couplings of the charged and of the neutral pions to the nucleon. One should not forget that, aiming at providing an explanation of the unexpected result of Ref. [3], Piekarewicz had (already in 1995) attributed the isospin-breaking effects to changes in the coupling constant due to the mass difference between the  $u$  and the  $d$  quarks [26]. In this context, we have also reported changes in the fitted value of the  $\pi N$  coupling constant when involving the CX data in the optimization, see Table 4 in Ref. [5].

The effects, shown in Figs. 4-6 and in Table 5 of this work, are systematic and indicative of the non-fulfillment of at least one of the three conditions (a)-(c), listed in the beginning of this section. One of the safest conclusions, drawn from Figs. 1-3, is that our approach yields results which closely represent and reproduce the bulk of the  $\pi N$  measurements for  $T \leq 100$  MeV; the low-energy behavior of the WI08 solution does not appear to account for the bulk of the low-energy data as successfully. If future investigation in the  $\pi N$  sector reveals that the meson-factory, low-energy experiments had been affected by severe energy-dependent systematic effects, then a solution based on a dispersion-relation analysis framework (like WI08) may be more reliable than ours. We will not speculate on how such effects could affect the two ES processes in one way (i.e., resulting in a systematic underestimation of the relevant DCSs) and the CX reaction in another (i.e., resulting in a systematic overestimation of the relevant DCSs). If, on the other hand, the persistent discrepancies, observed in the  $\pi N$  interaction at low energy, are to be blamed elsewhere (i.e., on a departure from a theoretical constraint or assumption), then our approach will be proven justified.

A final word on the subject of the EM corrections is due. In every PWA of the  $\pi N$  data, the goal is the extraction of the hadronic components of the partial-wave amplitudes, and of the hadronic phase shifts derived thereof. At the present time, no unique scheme exists for the removal of the EM effects from the  $\pi N$  data. Additionally, it is not always clear which EM corrections have been applied in the various PWAs which are available. The NORDITA corrections [21,22,23] were obtained in the 1970s, at a time when the meson factories were under construction; as a result, they do not include any of the data sets which became available after the meson factories came into operation. Part of our research programme in the late 1990s was the re-assessment of the EM effects at low energy [19,20]. To the best of our knowledge, the compatibility of these (and, perhaps, also other) EM-correction schemes has not been properly addressed; a comparison has been pursued in Ref. [27], yet only for a small subset of the available low-energy data.

In most works in the  $\pi N$  domain, fits of hadronic models are directly performed to the results of the PWAs of the  $\pi N$  data (partial-wave amplitudes and phase

shifts), assuming that these results represent ‘purely hadronic’ quantities. We stress that, so long as residual EM effects are still contained in the important results of the various PWAs (e.g., in the phase-shift solutions), no physical quantities which are estimated on their basis can be considered to be purely hadronic. The hope is that the values of the hadronic quantities are not much different from the current estimates, but this hope rests upon the assumption that the residual EM effects in the output of the various PWAs are small, which needs checking. As a result, when analyzing the data or when fitting to the output of any PWA of the  $\pi N$  data, one must always bear in mind that the available schemes, purporting at the removal of the EM effects, are neither complete nor model-independent. We believe that an innovative approach, aiming at the re-assessment of the EM effects in the  $\pi N$  domain, would be welcomed. The EM effects must be obtained in one consistent scheme for all three reactions and for an extensive energy range, i.e., from the  $\pi N$  threshold to the GeV region.

## Acknowledgements

We would like to thank I. I. Strakovsky for clarifying some questions regarding the output of the SAID Analysis Program. We acknowledge a helpful exchange of electronic mail with G. A. Miller on the subject of the violation of isospin invariance in the  $NN$  interaction.

## References

- [1] R. A. Arndt, W. J. Briscoe, I. I. Strakovsky, R. L. Workman, Extended partial-wave analysis of  $\pi N$  scattering data, Phys. Rev. C 74 (2006) 045205; SAID Analysis Program: <http://gwdac.phys.gwu.edu>.
- [2] R. A. Arndt, L. D. Roper, The use of partial-wave representations in the planning of scattering measurements. Application to 330 MeV  $np$  scattering, Nucl. Phys. B 50 (1972) 285–300.
- [3] W. R. Gibbs, Li Ai, W. B. Kaufmann, Isospin breaking in low-energy pion-nucleon scattering, Phys. Rev. Lett. 74 (1995) 3740–3743.
- [4] E. Matsinos, Isospin violation in the  $\pi N$  system at low energies, Phys. Rev. C 56 (1997) 3014–3025.
- [5] E. Matsinos, G. Rasche, Analysis of the low-energy  $\pi^- p$  charge-exchange data, Int. J. Mod. Phys. A 28 (2013) 1350039.
- [6] E. Matsinos, G. Rasche, Aspects of the ETH model of the pion-nucleon interaction, Nucl. Phys. A 927 (2014) 147–194.

- [7] F. James, ‘MINUIT - Function Minimization and Error Analysis’, CERN Program Library Long Writeup D506.
- [8] E. Matsinos, G. Rasche, Analysis of the low-energy  $\pi^\pm p$  elastic-scattering data, *J. Mod. Phys.* 3 (2012) 1369–1387.
- [9] H. Denz et al.,  $\pi^\pm p$  differential cross sections at low energies, *Phys. Lett. B* 633 (2006) 209–213.
- [10] H. Denz, Ph.D. dissertation, Tübingen University, 2004; <https://publikationen.uni-tuebingen.de/xmlui/handle/10900/48622>.
- [11] E. Matsinos, G. Rasche, Analysis of the low-energy  $\pi^\pm p$  differential cross sections of the CHAOS Collaboration, *Nucl. Phys. A* 903 (2013) 65–80.
- [12] E. Matsinos, G. Rasche, New analysis of the low-energy  $\pi^\pm p$  differential cross-sections of the CHAOS Collaboration, *Int. J. Mod. Phys. E* 24 (2015) 1550050.
- [13] R. Meier et al., Low energy analyzing powers in pion-proton elastic scattering, *Phys. Lett. B* 588 (2004) 155–162.
- [14] J. C. Bernauer et al., A1 Collaboration, Electric and magnetic form factors of the proton, *Phys. Rev. C* 90 (2014) 015206.
- [15] S. Venkat, J. Arrington, G. A. Miller, Xiaohui Zhan, Realistic transverse images of the proton charge and magnetization densities, *Phys. Rev. C* 83 (2011) 015203.
- [16] J. Arrington, W. Melnitchouk, J. A. Tjon, Global analysis of proton elastic form factor data with two-photon exchange corrections, *Phys. Rev. C* 76 (2007) 035205.
- [17] S. R. Amendolia et al., NA7 Collaboration, A measurement of the space-like pion electromagnetic form factor, *Nucl. Phys. B* 277 (1986) 168–196.
- [18] K. A. Olive et al., Particle Data Group, The review of particle physics, *Chin. Phys. C* 38 (2014) 090001.
- [19] A. Gashi, E. Matsinos, G. C. Oades, G. Rasche, W. S. Woolcock, Electromagnetic corrections to the hadronic phase shifts in low energy  $\pi^+ p$  elastic scattering, *Nucl. Phys. A* 686 (2001) 447–462.
- [20] A. Gashi, E. Matsinos, G. C. Oades, G. Rasche, W. S. Woolcock, Electromagnetic corrections for the analysis of low energy  $\pi^- p$  scattering data, *Nucl. Phys. A* 686 (2001) 463–477.
- [21] B. Tromborg, S. Waldestrøm, I. Øverbø, Electromagnetic corrections to  $\pi^+ p$  scattering, *Ann. Phys.* 100 (1976) 1–36.
- [22] B. Tromborg, S. Waldestrøm, I. Øverbø, Electromagnetic corrections to  $\pi N$  scattering, *Phys. Rev. D* 15 (1977) 725–729.
- [23] B. Tromborg, S. Waldestrøm, I. Øverbø, Electromagnetic corrections in hadron scattering, with application to  $\pi N \rightarrow \pi N$ , *Helv. Phys. Acta* 51 (1978) 584–607.

- [24] G. A. Miller, A. K. Oppen, E. J. Stephenson, Charge symmetry breaking and QCD, *Annu. Rev. Nucl. Part. S.* 56 (2006) 253–292.
- [25] V. A. Babenko, N. M. Petrov, Study of the charge dependence of the pion-nucleon coupling constant on the basis of data on low-energy nucleon-nucleon interactions, *Phys. Atom. Nucl.* 79 (2016) 67–71.
- [26] J. Piekarewicz, Isospin violations in the pion-nucleon system, *Phys. Lett. B* 358 (1995) 27–33.
- [27] W. R. Gibbs, R. Arceo, Minimal electromagnetic and mass difference corrections in  $\pi N$  scattering, *Phys. Rev. C* 72 (2005) 065205.

**Table 1**

The current values of the physical constants, used in this analysis. These values have been taken from the 2014 compilation of the Particle-Data Group [18]. Regarding the Roper resonance  $N(1440)$ , the partial width  $\Gamma_R$  of Section 2.1.2 is the product of the total width  $\Gamma_T$  and the corresponding branching ratio  $\eta$  for the  $\pi N$  decay modes of the resonance.

Physical quantity (unit)	Value
Charged-pion mass (MeV)	139.57018
Proton mass $m_p$ (MeV)	938.272046
$\Delta(1232)$ mass $m_\Delta$ (MeV)	1232
$\Delta(1232)$ decay width $\Gamma_\Delta$ (MeV)	117
$N(1440)$ $M_R$ (MeV)	1440
$N(1440)$ $\Gamma_T$ (MeV)	300
$N(1440)$ $\eta$	0.650

**Table 2**

The data sets comprising the truncated  $\pi^+p$  database, the pion laboratory kinetic energy  $T_j$  of the data set (in MeV), the number of degrees of freedom  $N_j$  after the removal of the outliers, the scale factor  $z_j$  which minimizes  $\chi_j^2$  of Eq. (5), the normalization uncertainty  $\delta z_j$  (reported by the experimental group or, if not reported, assigned by us, e.g., as the case is for the AULD79 data set), the value of  $(\chi_j^2)_{\min}$ , and the p-value of the fit. In the case of free floating,  $z_j$  is equal to  $\hat{z}_j$  of Eq. (9). The numbers in this table correspond to the final fit to the data using the  $K$ -matrix parameterizations of Section 2.1.1.

Data set	$T_j$	$N_j$	$z_j$	$\delta z_j$	$(\chi_j^2)_{\min}$	p-value	Comments
Differential cross sections							
AULD79	47.90	11	1.0290	0.1097	16.4530	0.1251	
RITCHIE83	65.00	8	1.0469	0.0240	18.2215	0.0196	
RITCHIE83	72.50	10	1.0062	0.0200	4.7931	0.9046	
RITCHIE83	80.00	10	1.0289	0.0140	18.9749	0.0406	
RITCHIE83	95.00	10	1.0308	0.0150	12.1585	0.2746	
FRANK83	29.40	28	1.0423	0.0370	19.3186	0.8880	
FRANK83	49.50	28	1.0581	0.2030	34.4110	0.1877	
FRANK83	69.60	27	0.9304	0.0950	23.2937	0.6691	
FRANK83	89.60	27	0.8603	0.0470	29.1001	0.3561	
BRACK86	66.80	4	0.8941	0.0120	2.4056	0.6616	freely floated
BRACK86	86.80	8	0.9368	0.0140	16.3766	0.0373	freely floated
BRACK86	91.70	5	0.9726	0.0120	12.5697	0.0278	
BRACK86	97.90	5	0.9709	0.0150	7.6323	0.1777	
BRACK88	66.80	6	0.9488	0.0210	10.6388	0.1002	
BRACK88	66.80	6	0.9574	0.0210	9.3760	0.1535	
WIEDNER89	54.30	19	0.9894	0.0304	14.8601	0.7314	
BRACK90	30.00	5	1.1805	0.0360	8.4943	0.1310	freely floated
BRACK90	45.00	8	1.0258	0.0220	8.4449	0.3913	
BRACK95	87.10	8	0.9717	0.0220	13.8636	0.0854	
BRACK95	98.10	8	0.9796	0.0200	15.0499	0.0582	
JORAM95	45.10	9	0.9712	0.0330	17.8659	0.0368	124.42° removed
JORAM95	68.60	9	1.0516	0.0440	9.1437	0.4241	
JORAM95	32.20	20	1.0224	0.0340	31.2306	0.0522	
JORAM95	44.60	18	0.9621	0.0340	27.6309	0.0679	30.74°, 35.40° removed

**Table 2 continued**

Data set	$T_j$	$N_j$	$z_j$	$\delta z_j$	$(\chi_j^2)_{\min}$	p-value	Comments
Analyzing powers							
SEVIOR89	98.00	6	1.0128	0.0740	5.5312	0.4777	
WIESER96	68.34	3	0.9100	0.0500	4.5009	0.2122	
WIESER96	68.34	4	0.9316	0.0500	4.7278	0.3164	
MEIER04	57.20-87.20	12	0.9824	0.0350	13.9222	0.3057	
MEIER04	45.20, 51.20	6	0.9709	0.0350	7.4638	0.2801	
MEIER04	57.30-87.20	7	1.0038	0.0350	11.0607	0.1360	
Partial-total cross sections							
KRISS97	39.80	1	1.0144	0.0300	2.5847	0.1079	
KRISS97	40.50	1	1.0023	0.0300	0.2646	0.6070	
KRISS97	44.70	1	1.0042	0.0300	0.1939	0.6597	
KRISS97	45.30	1	1.0053	0.0300	0.2402	0.6241	
KRISS97	51.10	1	1.0265	0.0300	4.1742	0.0410	
KRISS97	51.70	1	1.0046	0.0300	0.1507	0.6979	
KRISS97	54.80	1	1.0111	0.0300	0.3650	0.5457	
KRISS97	59.30	1	1.0294	0.0300	1.7134	0.1905	
KRISS97	66.30	2	1.0523	0.0300	4.4518	0.1080	
KRISS97	66.80	2	1.0077	0.0300	0.6370	0.7272	
KRISS97	80.00	1	1.0135	0.0300	0.3320	0.5645	
KRISS97	89.30	1	1.0074	0.0300	0.2509	0.6164	
KRISS97	99.20	1	1.0541	0.0300	3.9747	0.0462	
FRIEDMAN99	45.00	1	1.0467	0.0600	2.7169	0.0993	
FRIEDMAN99	52.10	1	1.0217	0.0600	0.3985	0.5279	
FRIEDMAN99	63.10	1	1.0401	0.0600	0.5992	0.4389	
FRIEDMAN99	67.45	2	1.0546	0.0600	1.3394	0.5119	
FRIEDMAN99	71.50	2	1.0508	0.0600	0.8682	0.6479	
FRIEDMAN99	92.50	2	1.0411	0.0600	0.5389	0.7638	

**Table 2 continued**

Data set	$T_j$	$N_j$	$z_j$	$\delta z_j$	$(\chi_j^2)_{\min}$	p-value	Comments
Total-nuclear cross sections							
CARTER71	71.60	1	1.0940	0.0600	2.7880	0.0950	
CARTER71	97.40	1	1.0475	0.0600	0.6326	0.4264	
PEDRONI78	72.50	1	1.0126	0.0600	0.1451	0.7033	
PEDRONI78	84.80	1	1.0302	0.0600	0.3085	0.5786	
PEDRONI78	95.10	1	1.0215	0.0600	0.1766	0.6743	
PEDRONI78	96.90	1	1.0154	0.0600	0.1132	0.7365	

**Table 3**

The equivalent of Table 2 for the fits to our  $\pi^-p$  elastic-scattering database. The numbers of this table correspond to the final fit to the data using the  $K$ -matrix parameterizations of Section 2.1.2.

Data set	$T_j$	$N_j$	$z_j$	$\delta z_j$	$(\chi_j^2)_{\min}$	p-value	Comments
Differential cross sections							
FRANK83	29.40	28	0.9841	0.0350	30.9946	0.3173	15.55° removed, freely floated
FRANK83	49.50	28	1.0985	0.0780	29.4176	0.3916	
FRANK83	69.60	27	1.0921	0.2530	24.7552	0.5882	
FRANK83	89.60	27	0.9457	0.1390	24.8611	0.5822	
BRACK86	66.80	5	0.9974	0.0130	13.9614	0.0159	
BRACK86	86.80	5	1.0031	0.0120	1.3828	0.9262	
BRACK86	91.70	5	0.9962	0.0120	3.0724	0.6888	
BRACK86	97.90	5	0.9998	0.0120	5.9607	0.3101	
WIEDNER89	54.30	18	1.1567	0.0304	23.5424	0.1706	
BRACK90	30.00	5	1.0210	0.0200	5.0513	0.4096	
BRACK90	45.00	9	1.0512	0.0220	11.6945	0.2311	36.70° removed
BRACK95	87.50	6	0.9812	0.0220	10.6655	0.0993	
BRACK95	98.10	7	1.0072	0.0210	8.4645	0.2934	
JORAM95	32.70	4	0.9941	0.0330	3.9286	0.4158	
JORAM95	32.70	2	0.9533	0.0330	5.6499	0.0593	
JORAM95	45.10	4	0.9540	0.0330	12.5594	0.0136	
JORAM95	45.10	3	0.9450	0.0330	9.5406	0.0229	
JORAM95	68.60	7	1.0829	0.0440	14.3284	0.0456	
JORAM95	68.60	3	1.0322	0.0440	2.3004	0.5124	
JORAM95	32.20	20	1.0615	0.0340	21.3464	0.3770	
JORAM95	44.60	20	0.9434	0.0340	30.3198	0.0648	
JANOUSCH97	43.60	1	1.0395	0.1500	0.1482	0.7002	
JANOUSCH97	50.30	1	1.0320	0.1500	0.1189	0.7302	
JANOUSCH97	57.30	1	1.0829	0.1500	4.7450	0.0294	
JANOUSCH97	64.50	1	1.0212	0.1500	0.0298	0.8629	
JANOUSCH97	72.00	1	1.2988	0.1500	4.6476	0.0311	

**Table 3 continued**

Data set	$T_j$	$N_j$	$z_j$	$\delta z_j$	$(\chi_j^2)_{\min}$	p-value	Comments
Analyzing powers							
ALDER83	98.00	6	1.0103	0.0400	5.3078	0.5050	
SEVIOR89	98.00	5	0.9871	0.0740	1.7012	0.8887	
HOFMAN98	86.80	11	1.0019	0.0300	5.9941	0.8738	
PATTERSON02	57.20	10	0.9468	0.0370	10.5993	0.3896	
PATTERSON02	66.90	9	0.9988	0.0370	4.6096	0.8669	
PATTERSON02	66.90	10	0.9522	0.0370	16.4217	0.0882	
PATTERSON02	87.20	11	0.9835	0.0370	8.1202	0.7025	
PATTERSON02	87.20	11	0.9944	0.0370	4.9386	0.9341	
PATTERSON02	98.00	12	0.9950	0.0370	6.5960	0.8831	
MEIER04	67.30, 87.20	3	0.9929	0.0350	3.2264	0.3580	

**Table 4**

The equivalent of Table 2 for the fits to our  $\pi^-p$  charge-exchange database. The numbers of this table correspond to the final fit to the data using the  $K$ -matrix parameterizations of Section 2.1.2.

Data set	$T_j$	$N_j$	$z_j$	$\delta z_j$	$(\chi_j^2)_{\min}$	p-value	Comments
Differential cross sections							
DUCLOS73	22.60	1	0.9422	0.0800	1.2111	0.2711	
DUCLOS73	32.90	1	0.9715	0.0800	0.2741	0.6006	
DUCLOS73	42.60	1	0.9100	0.0800	2.3763	0.1232	
FITZGERALD86	32.48	2	1.5008	0.0780	2.3360	0.3110	freely floated
FITZGERALD86	36.11	2	1.7161	0.0780	1.2144	0.5449	freely floated
FITZGERALD86	40.26	2	1.8332	0.0780	6.5440	0.0379	freely floated
FITZGERALD86	47.93	2	1.4509	0.0780	1.6502	0.4382	freely floated
FITZGERALD86	51.78	3	1.1216	0.0780	7.2398	0.0646	
FITZGERALD86	55.58	3	1.0933	0.0780	2.5533	0.4657	
FITZGERALD86	63.21	3	1.0548	0.0780	1.3372	0.7203	
FRLEZ98	27.50	6	1.0904	0.0870	10.4326	0.1076	
ISENHOWER99	10.60	4	1.0196	0.0600	2.1628	0.7058	
ISENHOWER99	10.60	5	1.0054	0.0400	1.4569	0.9180	
ISENHOWER99	10.60	6	1.0176	0.0400	8.0670	0.2332	
ISENHOWER99	20.60	5	0.9799	0.0400	1.5691	0.9050	
ISENHOWER99	20.60	6	1.0120	0.0400	8.1842	0.2249	
ISENHOWER99	39.40	4	1.0707	0.0600	7.3129	0.1202	
ISENHOWER99	39.40	5	1.0593	0.0400	8.4695	0.1322	
ISENHOWER99	39.40	5	0.9521	0.0400	5.1290	0.4003	
SADLER04	63.86	20	0.9540	0.0650	16.2394	0.7017	
SADLER04	83.49	20	0.9877	0.0520	11.7013	0.9260	
SADLER04	94.57	20	1.0303	0.0450	7.2943	0.9956	
JIA08	34.37	4	0.8433	0.1000	4.9400	0.2935	
JIA08	39.95	4	0.8676	0.1000	3.1953	0.5257	
JIA08	43.39	4	0.8780	0.1000	2.5106	0.6427	
JIA08	46.99	4	0.9799	0.1000	5.1602	0.2713	

**Table 4 continued**

Data set	$T_j$	$N_j$	$z_j$	$\delta z_j$	$(\chi_j^2)_{\min}$	p-value	Comments
Differential cross sections							
JIA08	54.19	4	0.9057	0.1000	2.1191	0.7139	
JIA08	59.68	4	0.9318	0.1000	3.0789	0.5447	
MEKTEROVIC09	33.89	20	1.0239	0.0340	17.0108	0.6523	
MEKTEROVIC09	39.38	20	1.0145	0.0260	14.7679	0.7895	
MEKTEROVIC09	44.49	20	1.0100	0.0270	33.1582	0.0324	
MEKTEROVIC09	51.16	20	1.0355	0.0290	15.0640	0.7727	
MEKTEROVIC09	57.41	20	1.0390	0.0290	19.4998	0.4896	
MEKTEROVIC09	66.79	20	1.0227	0.0300	19.5380	0.4871	
MEKTEROVIC09	86.62	20	1.0016	0.0290	31.0086	0.0551	
Legendre expansion of the differential cross section							
SALOMON84	27.40	3	0.9722	0.0310	2.7669	0.4290	
SALOMON84	39.30	3	0.9939	0.0310	1.0926	0.7789	
BAGHERI88	45.60	3	1.0055	0.0310	0.1372	0.9870	
BAGHERI88	62.20	3	0.9582	0.0310	3.6125	0.3065	
BAGHERI88	76.40	3	0.9725	0.0310	3.3190	0.3450	
BAGHERI88	91.70	3	1.0151	0.0310	2.8312	0.4184	
Measurement of the width of pionic hydrogen							
SCHROEDER01	0.00	1	0.9746	0.0225	2.5283	0.1118	
Analyzing powers							
STASKO93	100.00	4	0.9944	0.0440	1.4508	0.8353	
GAULARD99	98.10	6	1.0234	0.0450	1.0835	0.9823	

**Table 4 continued**

Data set	$T_j$	$N_j$	$z_j$	$\delta z_j$	$(\chi_j^2)_{\min}$	p-value	Comments
Total cross sections							
BUGG71	90.90	1	1.0226	0.0600	0.1478	0.7007	
BREITSCHOPF06	38.90	1	0.9960	0.0300	0.1641	0.6854	
BREITSCHOPF06	43.00	1	1.0011	0.0300	0.0259	0.8722	
BREITSCHOPF06	47.10	1	0.9980	0.0300	0.0578	0.8100	
BREITSCHOPF06	55.60	1	0.9951	0.0300	0.2131	0.6444	
BREITSCHOPF06	64.30	1	0.9724	0.0300	3.8191	0.0507	
BREITSCHOPF06	65.90	1	0.9777	0.0300	2.3820	0.1227	
BREITSCHOPF06	76.10	1	0.9812	0.0300	1.6410	0.2002	
BREITSCHOPF06	96.50	1	0.9819	0.0300	0.5924	0.4415	

**Table 5**

The fitted values of the parameters of the weighted linear fit to the data shown in Figs. 4-7, as well as their uncertainties, corrected with the Birge factor  $\sqrt{\chi^2/\text{NDF}}$ , taking account of the goodness of each fit.

Reaction	Intercept	Slope ( $10^{-3} \text{ MeV}^{-1}$ )
$\pi^+p$	$0.936 \pm 0.028$	$0.70 \pm 0.34$
$\pi^-p$ elastic-scattering	$0.972 \pm 0.021$	$0.16 \pm 0.27$
$\pi^-p$ charge-exchange	$1.041 \pm 0.019$	$-0.43 \pm 0.34$
All three $\pi N$ reactions	$0.985 \pm 0.014$	$0.10 \pm 0.18$

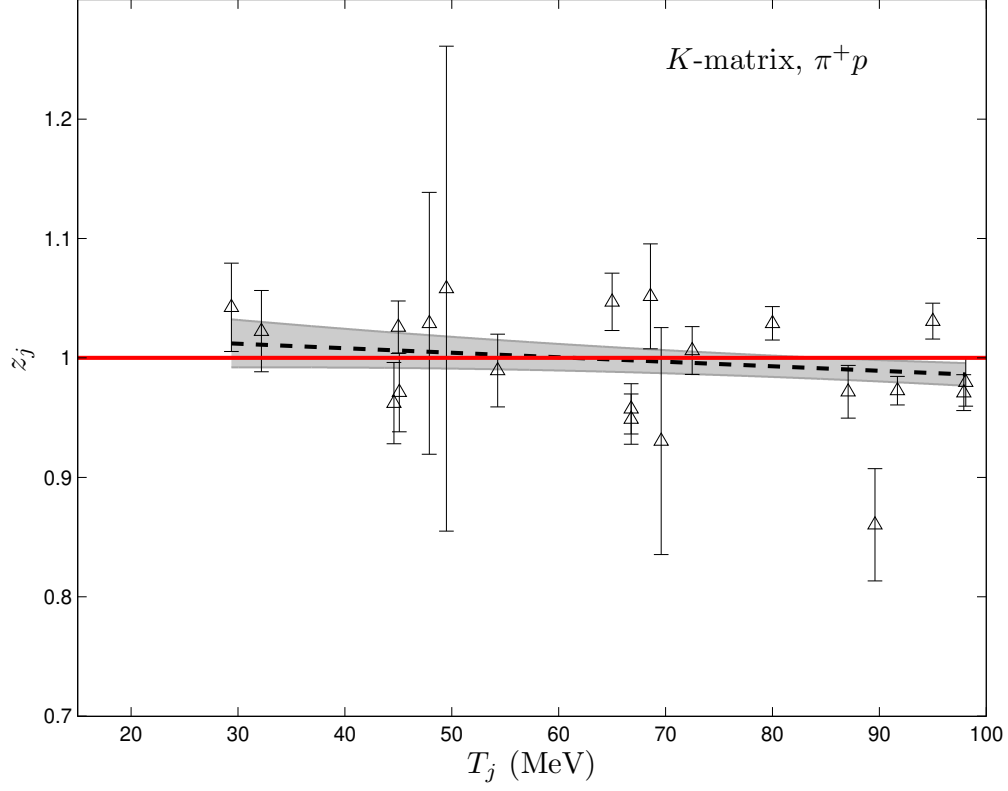


Fig. 1. Plot of the scale factors  $z_j$  which minimize  $\chi_j^2$  of Eq. (5) for the fits to our low-energy  $\pi^+p$  database using the  $K$ -matrix parameterizations of Section 2.1.1;  $T_j$  denotes the pion laboratory kinetic energy of the  $j$ -th experiment. The data correspond to DCSs only; the data sets which had to be freely floated are not shown. The dashed straight line represents the optimal, weighted linear fit to the data shown and the shaded band  $1\sigma$  uncertainties around the fitted values. The red line is the optimal, unbiased outcome of the optimization.

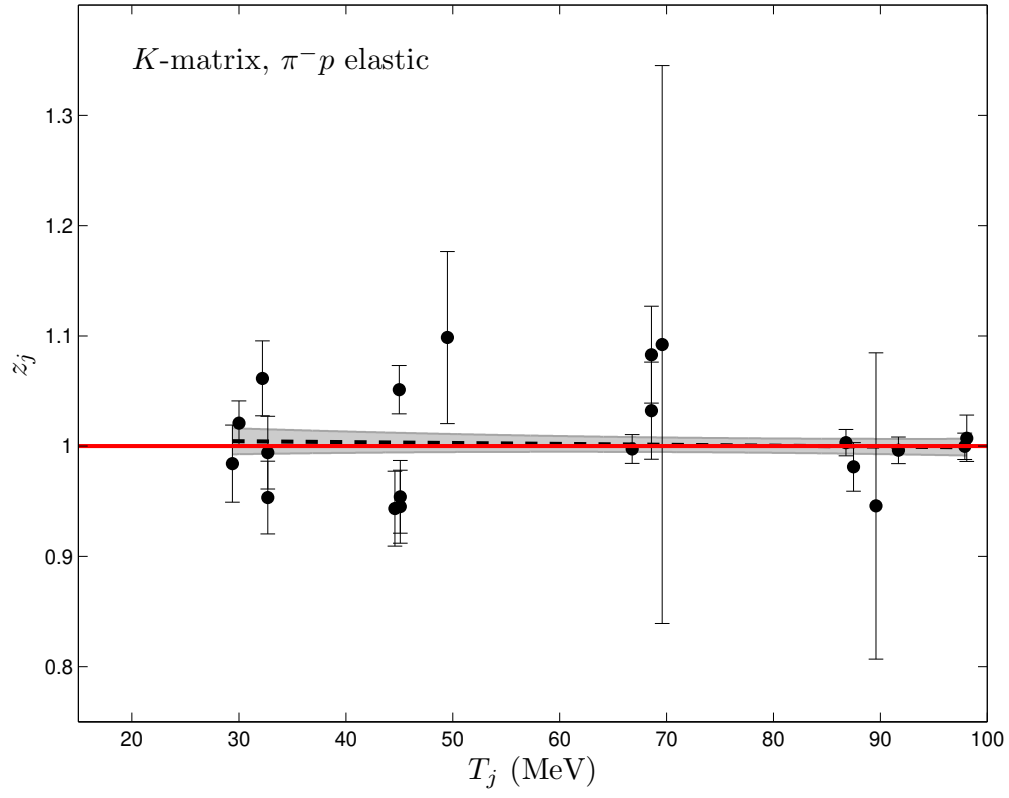


Fig. 2. The equivalent of Fig. 1 for the fits to our  $\pi^-p$  elastic-scattering database.

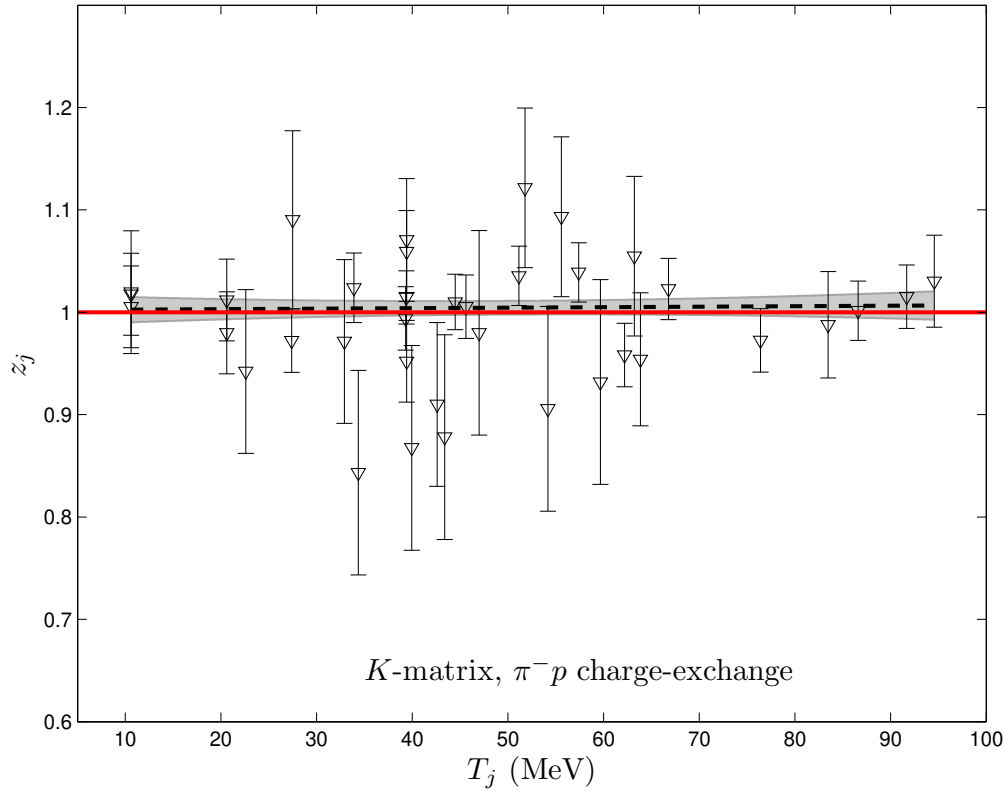


Fig. 3. The equivalent of Fig. 1 for the fits to our  $\pi^- p$  charge-exchange database.

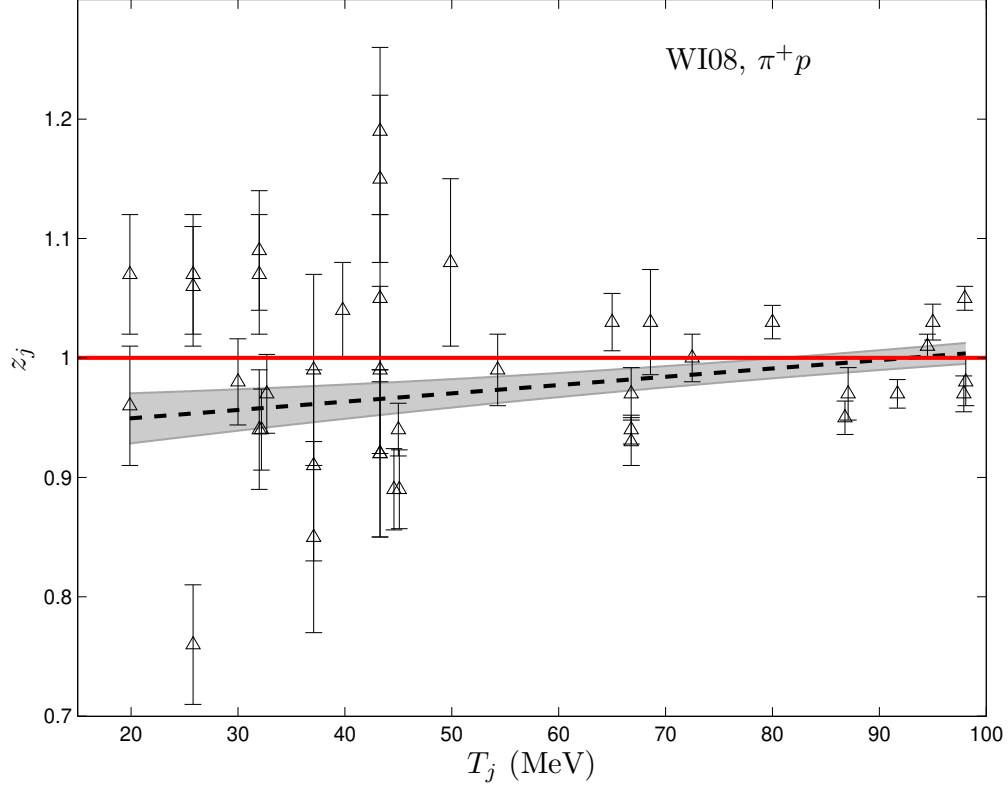


Fig. 4. Plot of the scale factors  $z_j$  which minimize  $\chi_j^2$  of Eq. (5) for the fits to the SAID low-energy  $\pi^+p$  database (yielding the WI08 solution);  $T_j$  denotes the pion laboratory kinetic energy of the  $j$ -th experiment. The data correspond to DCSs only; the data sets which were floated are not shown. The dashed straight line represents the optimal, weighted linear fit to the data shown (see Table 5) and the shaded band  $1\sigma$  uncertainties around the fitted values. The red line is the optimal, unbiased outcome of the optimization.

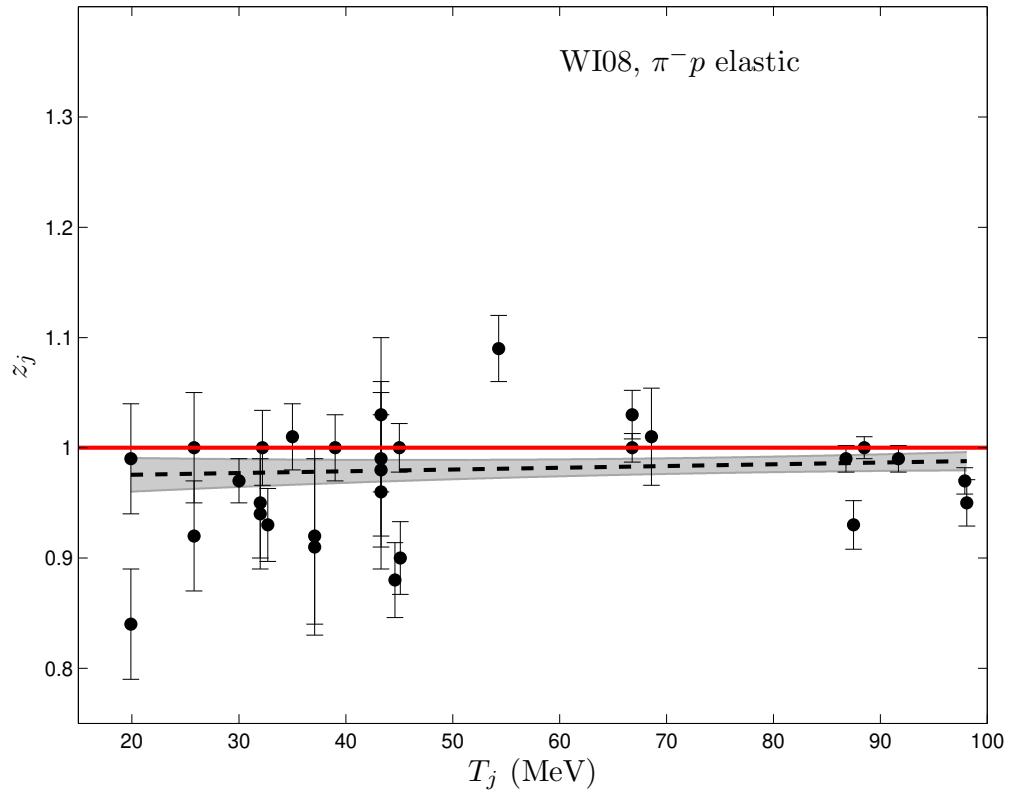


Fig. 5. The equivalent of Fig. 4 for the SAID low-energy  $\pi^-p$  elastic-scattering database.

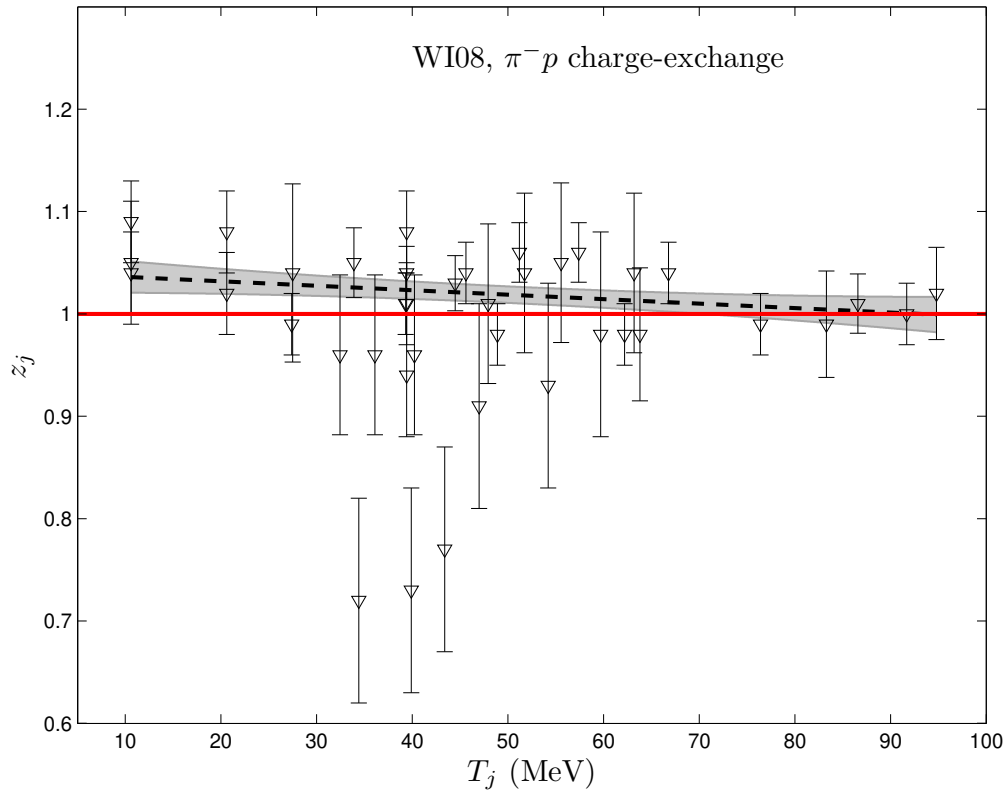


Fig. 6. The equivalent of Fig. 4 for the SAID low-energy  $\pi^- p$  charge-exchange database.

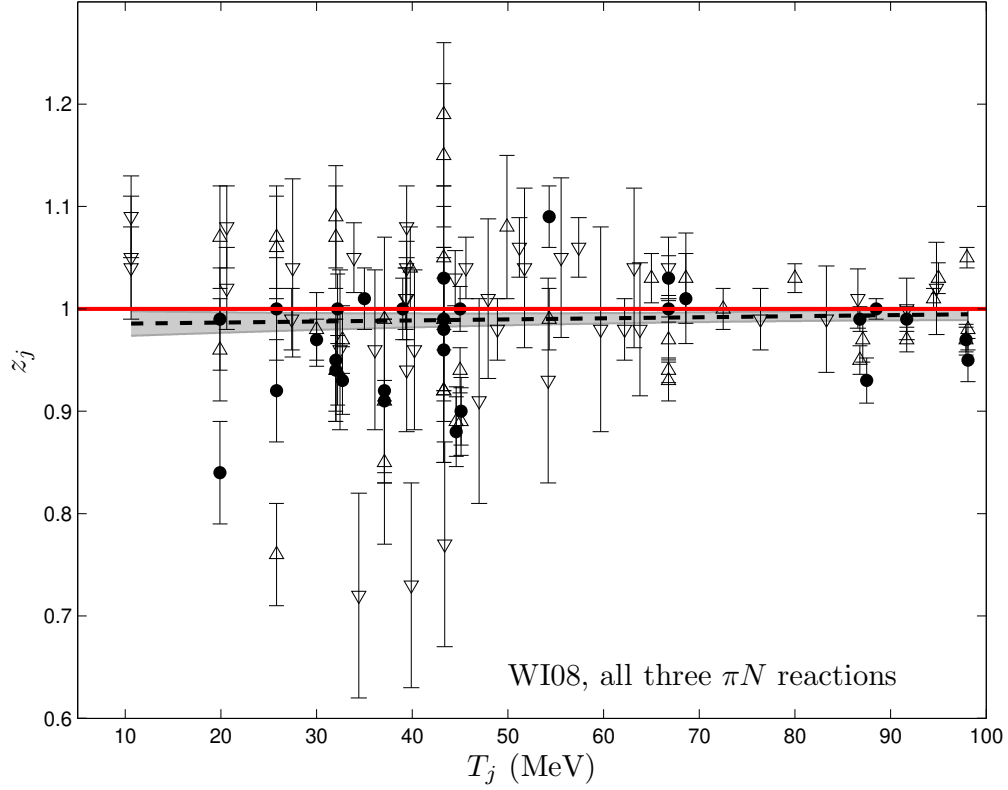


Fig. 7. Plot of the scale factors  $z_j$  which minimize  $\chi_j^2$  of Eq. (5) for the fits to the entire SAID low-energy  $\pi N$  database (yielding the WI08 solution);  $T_j$  denotes the pion laboratory kinetic energy of the  $j$ -th experiment. The data correspond to DCSs only (upward triangles:  $\pi^+p$ , dots:  $\pi^-p$  elastic, downward triangles:  $\pi^-p$  charge-exchange); the data sets which were floated are not shown. The dashed straight line represents the optimal, weighted linear fit to the data shown (see Table 5) and the shaded band  $1\sigma$  uncertainties around the fitted values. The red line is the optimal, unbiased outcome of the optimization.